The 20/20 telescope: MCAO imaging at the individual and combined foci

Roger Angel, Michael Lloyd-Hart, Keith Hege, Roland Sarlot and Chien Peng

Steward Observatory, The University of Arizona, Tucson, AZ 85721
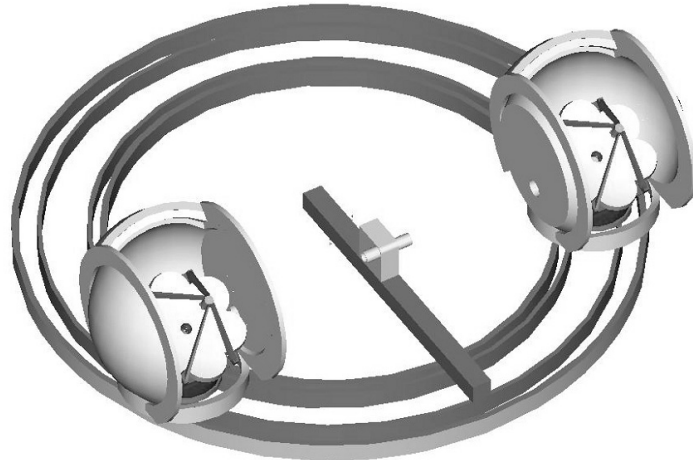
ABSTRACT

The 20/20 telescope is a new concept for the GSMT with two 21 m filled-aperture elements. It has the light collecting power of a single 30 m telescope, but by moving the two elements apart and combining their images coherently, it will be capable of higher resolution. To obtain a wide field of view at the combined focus, the two apertures must be maintained perpendicular to the source. This is achieved by their continuous motions about a 100 circular track.

Both the individual and combined foci will take advantage of multi-conjugate adaptive optics (MCAO) to obtain diffraction limited fields of ~ 1 arcminute. At the coherent, combined focus, the PSF is the Airy pattern of the individual telescope multiplied by Young's fringes. Adaptive correction of path length for one star in the MCAO field ensures a PSF with a stable, centered fringe for all stars in the field. Images are reconstructed using generalized Lucy-Richardson methods from exposures with different baseline angles and separations. The highest resolution is $4\times$ that of a 30 m telescope and the images, with the same number of resolution elements as a Palomar Schmidt plate, will be rich in detail. The combination of MCAO stabilized wavefronts and long baseline should result in astrometric accuracy of better than 10 μarcsec. The double aperture telescope is also ideal for Bracewell nulling interferometry for direct detection of extra-solar planets.

In this paper we give a preliminary but complete optical prescription for the individual telescopes, their MCAO relays with deformable mirrors conjugated to 0, 6 and 12 km, and for coherent combination of the MCAO fields for the closest separation. Wavefront measurements will be made from 5 sodium and 5 Rayleigh laser guide stars and 1 natural star at each telescope. Models which reconstruct tomographically the turbulence and make correction at DMs conjugated to just 0 and 6 km, show 50% Strehl over ≥ 1 arcmin field. The tomographic method will be tested at $\frac{1}{3}$ scale at the 6.5 m MMT telescope with just the 5 Rayleigh laser guide stars at 30 km. A similar level of correction is predicted.

Email: rangel@as.arizona.edu

1. INTRODUCTION TO 20/20

1.1. General Considerations

How should a Giant Segmented Mirror Telescope (GSMT) be built? A single round, filled aperture has the advantage of a simple Airy pattern, and high sensitivity to faint, isolated point sources. But for any given collecting area, a circular aperture also has the lowest resolution. A circular 30 m aperture, for example, would collect 6× as much light as the 23 m long Large Binocular Telescope (Angel et al. 1998), but would realize only a marginal improvement in resolution. Given that much of the scientific rationale for larger ground based telescopes rests on their capability to achieve high spatial resolution through adaptive optics, it is important to explore how this might be improved.

Our concept calls for separate telescopes with a combined, coherent focus. Multi-conjugate adaptive optics (MCAO) will be used to correct not only the individual apertures, but the combined focus as well, so it too can be diffraction limited over a substantial field of view. To best combine the simplicity and power of a large filled aperture with the higher resolution potential of a coherent phased array, we need the following:

1) There should be **just two filled apertures**. This is clearly preferred when the telescopes are to be operated separately, for then each one can deliver high resolution when operated with adaptive optics. But two apertures are also optimal for an adaptive coherent array. Unlike the case for radio interferometers, there is no advantage in using more telescopes. Phase-closure techniques that require 3 or more apertures are not needed for an adaptive coherent array, where the phase reference is derived from a natural star in the field. Because optical signals cannot be amplified, there is also no gain in correlating a larger number of apertures.

2) When two apertures are combined for true imaging with more than a factor two improvement in resolution, it is necessary to **vary the baseline spacing** between the two telescopes. Earth rotation changes the baseline angle, but if the length is fixed, as in the LBT, the center-to-center spacing can be no more than twice the mirror diameter for full u-v plane coverage. Higher resolution requires that wider separations be used in addition.

3) The **telescopes themselves must move during observations**. Wide MCAO fields can be combined coherently for higher resolution imaging relatively easily and efficiently, provided that the telescopes are tracked continuously so as to maintain the baseline perpendicular to the source. Wide-field imaging obtained in this way not only enables unique science programs, it ensures that suitable background stars can be found for real-time measurement of atmospheric path length errors, and for astrometric reference.

1.2. The 20/20 Concept

The 20/20 telescope is designed to satisfy these criteria. It has two telescopes mounted on a 100 m diameter track, each one 21 m in diameter for a total area is 700 m^2, the same as a 30 m single dish. They can be held stationary and operated independently as alt-azimuth telescopes when desired, with a wide seeing-limited field, or with correction to the 21 m diffraction limit made with an adaptive secondary and other deformable mirrors.

When higher resolution is needed, the telescopes are moved to the desired spacing and oriented so the baseline is normal to the source. The local azimuth motion is then stopped, and replaced by continuous motion of both telescopes around the 100 m track, with the light from both brought to a station kept midway between the telescopes. In this way the pathlengths remain constant and the baseline remains perpendicular to the source. The effect of Earth's rotation is to turn the baseline about the line of sight.

When beams individually corrected by AO are combined coherently, the PSF is given by the convolution of the Airy pattern of the individual 21 m apertures crossed by Young's fringes with separation λ/s where s is the center-to-center spacing. Atmospherically induced path differences will cause the fringe position or phase to jitter. However, if the fringe position is measured for one star in the field, and path length adjusted so as to center a fringe on the Airy pattern, then the fringes will be similarly positioned for all other objects in the isoplanatic patch (Hege et al. 1985, Shao & Colavita 1992, Esposito et al. 2000). This should hold true also for the larger fields corrected by MCAO. For the closest spacing, 30 m center-to center, the stabilized PSF shows three fringes across the Airy core, the strong central fringes containing 50% of all the energy collected by the two telescopes.

Because the PSF is stabilized, long integrations of faint objects can be recorded, provided the optical system does not itself introduce field-dependent path length differences, and there is an adequate field star for fringe tracking. We call this mode of operation **adaptive coherent imaging**. Its relationship to conventional interferometry is essentially the same as that of adaptive optics to speckle interferometry for single apertures. In both cases, without adaptive correction, diffraction-limited information can only be extracted from short
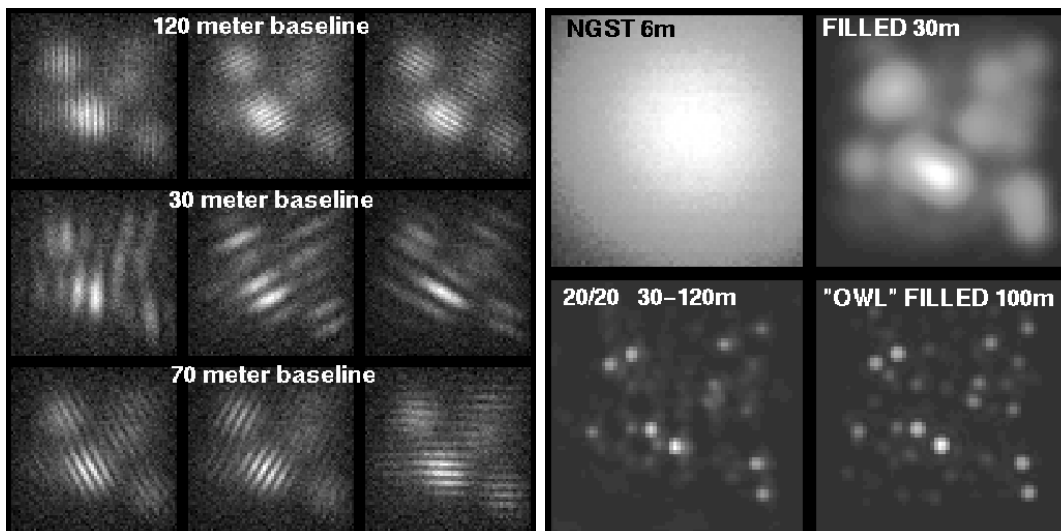
Figure 1. *a*) Simulated images of a tiny portion of a galactic bulge at 100 Mpc seen at 3 different baselines. *b*) Comparison of images of the bulge as seen by 4 different planned telescopes.

exposures that freeze atmospheric distortion, while with correction from a reference star, long exposures for diffraction-limited images of very faint field objects become possible. The required magnitude of the phase reference star is no brighter than is needed for tip/tilt reference for laser guide star AO; thus whenever adaptive wavefront correction is possible, so is adaptive coherent imaging.

The deconvolution of high resolution images from a set of 20/20 exposures will be along the lines already developed for imaging with the LBT (Hege et al. 1999, Correia & Richichi 2000, Bertero & Boccacci 2000). A paper describing the techniques with numerical modeling is in preparation by Keith Hege and Laird Close.

The full power of the telescope to obtain wide field images of faint fields at its limiting resolution (that of a 120 m filled aperture telescope) will require long integrations at several different baselines. The time will be justified for key deep field projects that can take advantage of uniquely high resolution images covering a wide field of view. The amount of detail in one deconvolved K band image will be the same as in a Palomar Schmidt plate. Raw K band images covering 1 arcminute will be recorded by a 50,000 $\times$ 50,000 pixel mosaic (possibly less in one dimension if an anamorphic relay is used.)

Details of a field covering the bulge of a galaxy at 100 Mpc modeled by L. Close are shown in Figure 1*a*. The model includes 1000 stars, most of which are too faint to show individually. The nine exposures are modeled for 20 hours each, at 3 different baselines and several different angles. Working from just these nine images, which include the effects of photon and read noise, K. Hege deconvolved the image shown in Figure 1*b*, with resolution 3.8 mas. The brightest star has K' magnitude 27.5, and photometry at K'=29 is good to 0.1 mag rms. We show also in the figure simulated images from filled 30 and 100 m aperture telescopes, for the same exposure time. The relatively poor resolution of the 30 m filled aperture results in photometric errors (0.3 mag for the brightest stars). The 100 m filled aperture has effectively no photon noise, but photometric errors of 0.07 mag are present because of residual confusion.

The challenge for adaptive correction of 20/20's individual apertures to the diffraction limit is not so great as for larger filled apertures, but already a single sodium laser guide star would be ineffective for 21 m aperture, even on-axis, because of the focus anisoplanatism. Multiple sodium lasers and atmospheric tomography will be used to overcome this problem, and will also lead naturally to a field substantially larger than for single-conjugate correction. We thus envisage that MCAO with multiple beacons for each telescope will be the standard high resolution mode of operation, except when the object under study is bright itself or close by a bright reference.

The actual realization of images with such detail and depth will require careful attention to the optical system. In this paper we focus on the optical design of 20/20, and the proposed implementation of the individual MCAO foci and their coherent combination. Section 2 gives details of the optics, including a complete prescription from the primary mirrors to the combined focus. Section 3 gives details of the manufacture of the primary and deformable mirror elements. Section 4 describes the laser guide star and tomography technique for MCAO at

20/20, and the 1/3 scale model we plan to test at the MMT, with Rayleigh beacons at 30 km providing the same sampling as sodium beacons at 95 km for the 21 m telescopes.
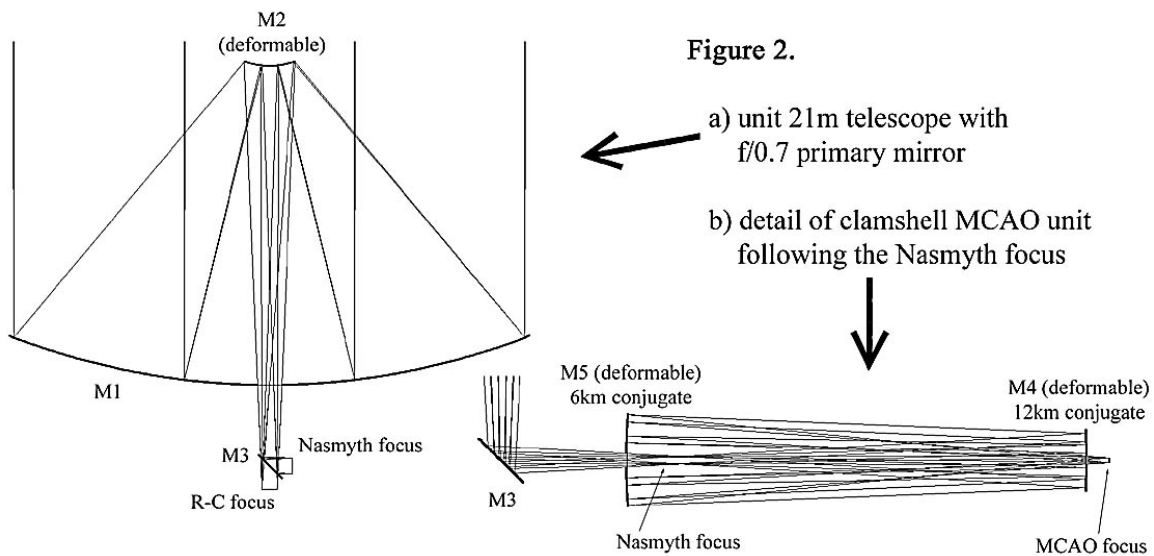
2. OPTICAL DESIGN

The preliminary but complete optical design provides for three foci with progressively higher degrees of correction. The basic 21 m unit telescopes are Ritchey Chretien, with an optional fold mirror on the elevation axis for Nasmyth instruments. The RC secondary is deformable, so these foci can be used for both seeing limited and single conjugate AO operation. MCAO foci with three conjugate correction are obtained by when desired by a clamshell relay consisting of two deformable mirrors which follows the Nasmyth focus. For coherent wide field imaging, the MCAO fields are relayed and made coincident at a central combined focus. These three stages are described below.

2.1. Ritchey-Chretien Foci

The high-resolution adaptive secondary mirrors will be similar to those used for the 6.5 m MMT and LBT telescopes. The actuator spacing projected to the entrance pupil will be 25 cm. The secondaries are conjugated effectively to the ground turbulence (actually to a plane 145 m below the primary vertex). We plan to use them in the near infrared to correct this component of wavefront aberration over a wide field. The servo will be based on the average wavefront measured for multiple natural stars across the field. In this way a reduction of typically 30% in seeing can be expected over fields of $\sim$ 10 arcminutes, depending on the strength of ground layer turbulence correctable with the secondary. Such improved images will be valuable for wide field imaging and for seeing-limited, multi-object or integral field spectroscopy

Full atmosphere adaptive correction with the secondaries, based on a suitably bright natural guide star, will work as for 8 m telescopes today, within the same size isoplanatic patch, independent of aperture. The adaptive secondaries are highly advantageous for the thermal infrared, yielding at the direct RC focus the lowest possible telescope thermal background for single-conjugate AO correction. The diffraction limited resolution at 10 μm, for example, will be 0.1 arcsec, and the single conjugate isoplanatic angle $\geq$ 1 arcminute.

The individual 21 m telescopes need to be compact and stiff, so they and their enclosures will resist wind buffering and can more easily be moved on tracks. We choose a primary focal ratio of f/0.7, used with a 2.2 m adaptive secondary to form Ritchey-Chretien and Nasmyth foci as illustrated in Figure 2a. The f/8.6 RC focus is located 4.6 m behind the primary vertex. (The full optical prescription is given in the table below, dimensions in mm.) Despite the fast primary, the field of view for seeing-limited imaging is quite large, 12 arcminutes with 80% of the energy in 1/3 arcsec diameter or less. The plate scale is 940 μm/arcsec. The removable Nasmyth flat is located on the elevation axis 3.6 m behind the primary vertex, in the style of a radio telescope.

Figure 2.

a) unit 21m telescope with f/0.7 primary mirror

b) detail of clamshell MCAO unit following the Nasmyth focus

Optic	Radius	Thickness	Glass	Diameter	Conic	r^4	r^6	r^8
					Ritchey-Chretien Telescope			
	Infinity	Infinity						
M1 pri.	-30741.89	-13903.72	Mirror	22450.0	-1.001343			
M2 0km DM	-3187.177	13903.72	Mirror	2172.357	-1.391236			
	Infinity	3600		577.9171				
	-	0		-		X tilt	45°	
M3 fold flat	Infinity	0	Mirror	255.5027				
	-	-1000		-		Y tilt	45°	
Nasmyth focus	Infinity	-3675		57.25579				
					MCAO Corrector			
M4 12km DM	23413.75	0	Mirror	491.1914	-461.7619	0	3.59E-18	-2.47E-23
	Infinity	3675		491.0925				
M5 6km DM	-5244.359	-3675	Mirror	775.3207	0.7620396	0	6.39E-19	-1.02E-24
MCAO focus	Infinity	-2214.533		36.89481				
					Coherent Image Combiner			
Collim. triplet	-5892.354	-35	BaF2	530				
Collim. triplet	1843.337	-99.90006		530				
Collim. triplet	-5547.171	-20	SF6	530				
Collim. triplet	-1944.841	-25.24318		530				
Collim. triplet	-2620.432	-35	BaF2	530				
Collim. triplet	2429.094	-5895.324		530				
Ext pupil	Infinity	0		441.7435				
	-	0		-		Y decen.	294.93	
Schmidt cor.	-238576.2	-40	F. Silica	1100				
Schmidt cor.	-46149.87	0		1100		3.01E-11	3.65E-18	0
Schmidt cor.	-46149.87	-40	F6	1100		3.01E-11	3.65E-18	0
Schmidt cor.	-134611.7	0		1100				
Schmidt cor.	-134611.7	-40	CaF2	1100				
Schmidt cor.	835227.5	0		1100				
	-	-1585.045		-		Y decen.	-294.93	
	-	0		-		X tilt	-45°	
M6 fold flat	Infinity	0	Mirror	666.0717				
	-	2000		-		X tilt	-45°	
	-	0		-		Y decen.	294.93	
M7 Schmidt pri.	-3637.463	-1803.347	Mirror	1088.626				
Combined focus	-1835.636			27.05462				

2.2. MCAO Foci

For the optical implementation of MCAO we plan to add a relay after the Nasmyth focus consisting of two additional curved deformable mirrors conjugated to 6 km and 12 km altitude (Figure 2b). This clamshell relay provides correction with the absolute minimum of additional optical surfaces. The first relay mirror, M4, 0.56 m in diameter and nearly flat, is at the 12 km conjugate formed directly by the RC telescope. The second relay mirror, M5, conjugated to 6 km, is 0.84 m diameter and concave with 5 m radius. Both deformable mirrors are, like the adaptive secondaries, curved and aspheric.

The relayed image, formed just beyond M4, is at f/5.15 at a plate scale of 567μm /arcsec. The 2 arcminute field is 53 mm in diameter, and the central pupil obscuration is less than 5% by area. The holes leave room for unvignetted transmission of the sodium laser beacons at 1 arcminute radius. The image quality for this optical system is diffraction-limited in the optical over l arcminute field. The sodium beacons reimaged through the MCAO optics suffer less than 0.1 arcsec blurring from spherical aberration, much less than their inherent size from seeing in the upward beams.
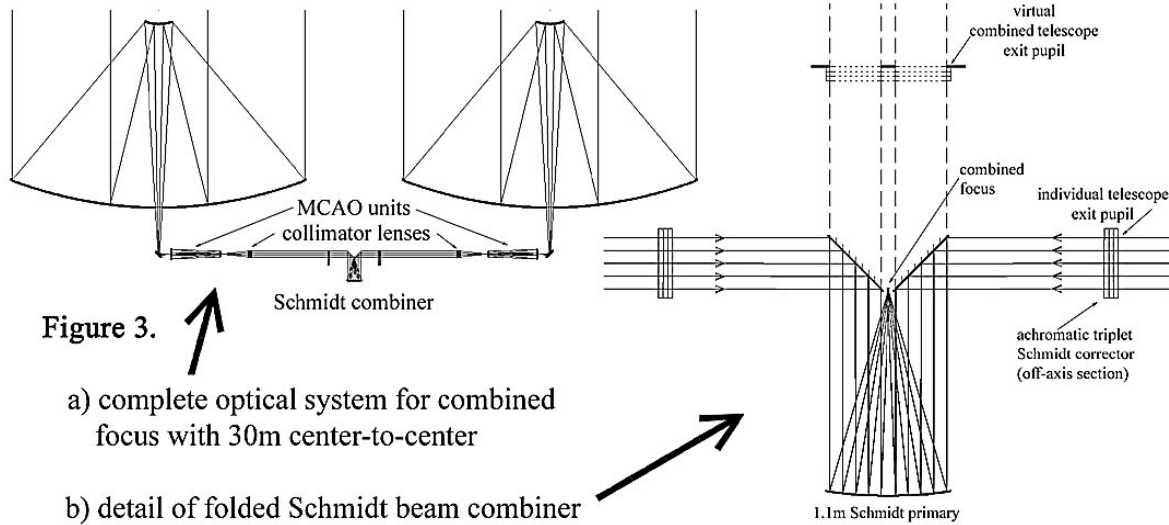
2.3. Preliminary Optical Design of the Short-baseline, Combined, Coherent Focus

20/20 requires optical systems to realize coherent combination of the individually corrected MCAO fields. For a constant PSF over the field, with a centered achromatic Young's fringe everywhere, there must be no difference between the optical paths to the center of each image in an overlapped pair. As is now well known, this requires

that the system exit pupil has the same geometry as the entrance pupil, and that distortion of the individual images be carefully controlled (Hege et al. 1985).

Previously, these conditions have been satisfied only in arrays in which the separate telescopes were rigidly mounted on the same structure. As we noted above, for 20/20 we plan to vary the center-to-center spacing of the two telescopes to obtain high resolution when desired. We have opted for three fixed spacings of 30, 65 and 100 m. These three are enough for deconvolution of ideal images (given rotation of the parallactic angle), since all baselines from 0–121 m are covered (0–52 m, 44–86 m and 79–121 m respectively). The three separate optical combination systems will be constructed. Their design is challenging, and is an ongoing activity.

We give here a preliminary but complete and functional design for a 30 m beam combiner (Figure 3a). The complete prescription is given in the table above. The MCAO foci are followed by achromatic (1.25–2.5μm) triplet collimators. These use elements of barium fluoride 0.5 m in diameter which are bigger than the present manufacturing limit, but an increase to this size is needed for many large telescope optics, and could be achieved. The exit pupils are formed at the entrance windows of the beam combining unit, which is separately translated to hold its position midway between the two telescopes. The entrance windows are sections cut from the achromatic corrector plate of a 1.1 m Schmidt camera. Folding mirrors as shown in the detail (Figure 3b) create the correct (virtual) exit pupil and leave room for a camera with no obscuration. The plate scale at the 1 arcminute (26 mm) combined image is 450 μm/arcsec.

Figure 3.

a) complete optical system for combined focus with 30m center-to-center

b) detail of folded Schmidt beam combiner

Standard optics design codes do not provide for calculation of diffraction limited PSFs allowing for interference in multi-aperture systems. ZEMAX does however output the point of intersection in the focal surface for each individual ray traced through a system, together with the optical path length and direction cosines at that point. From this information we calculate the path length to any neighboring point in the focal plane, and hence the path lengths of individual rays through different apertures to different points in the combined focal surface. The PSFs obtained for different field positions by summing and squaring complex amplitudes show clean beam profiles with centered achromatic fringes over a full 1 arcminute field (Figure 4).

The optical design is very efficient, in that the total number of mirror surfaces from the primary mirror to the coherent combined focus, including the primary, secondary and two additional deformable mirrors, is only seven. There are also six refracting elements in 4 groups, which would be antireflection coated. The folded Schmidt camera has the advantage of a nearly flat focal surface and clear access to the focal surface, but it does result in a rather fast focus with small images. The K band fringes are spaced by 15 mas or 6.75 μm. Sampling by four 15 μm pixels/fringe will require a camera with a magnification of $\sim 10\times$ magnification, to a 0.27 m diameter mosaic, 18,000 pixels across. Optical designs for longer wavelengths, and the two wider spacings are being studied.
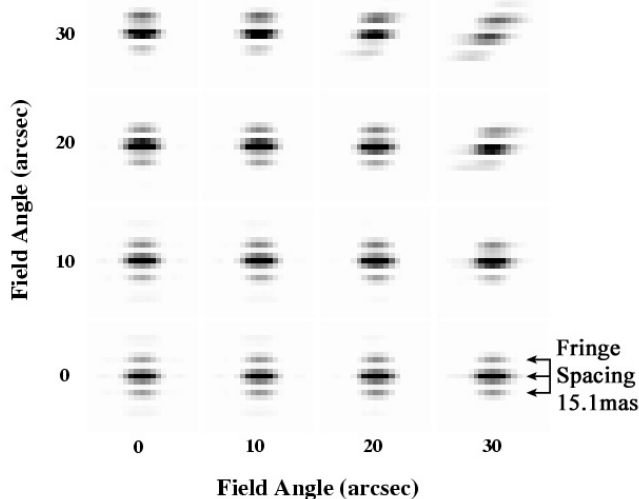
Figure 4. PSFs as a function of off-axis field position for the 30m beam combiner. A grid of 20×20 rays was used from the input pupil plane of each "arm" of the optical system. From the computed path lengths to a given focal plane position, a complex amplitude at wavelength 2.2 μm was derived for each path, and the intensity from the square of the summed amplitudes. Each PSF is shown as points on a local 4 mas pixel grid, magnified 185× relative to the scale field angle.

3. TELESCOPE STRUCTURE AND COMPENSATION FOR WIND MOTION

As telescope size is increased, the relative contribution of wind disturbance also increases (Woolf & Ulich 1984). To minimize these effects, we have made the telescopes as short and stiff as possible using LBT mechanical design experience (Del Vecchio et al. 1994). They will be protected by two co-moving enclosures, moving on a separate, wider track to minimize mechanical coupling. The preliminary finite element design includes hydrostatic bearings for independent azimuth rotation for each telescope as well as for motion around the 100 m track. The moving mass for each 21 m telescope is 850 tons, less than twice the mass of some current single 8 m telescopes, and the lowest resonant frequency stands currently at 5 Hz. The lowest modes are motions of the secondary support, presently modeled in steel. Improvement to 7 Hz should be possible by making the quadrupod support structure of carbon fiber composite. Wind induced path length errors are projected to be no larger than 1 mm because of the high stiffness.

Whatever dynamic wind induced wavefront and path length errors remain must be corrected by the adaptive optics system to a small fraction of a wavelength, along with the errors induced by atmospheric turbulence. In this section we outline the major optical and mechanical elements and this control strategy. The mechanical designs are by Warren Davison, and will be published elsewhere.

3.1. Primary Segment Configuration

The 21 m primary mirrors will be each made from seven large segments, a central hexagon with six surrounding petals. This configuration minimizes gap losses and phase steps that cause scatter and reduce contrast, important for exo-planet studies. Manufacture of the large segments will take advantage of the mature technology already developed for casting, polishing, supporting and coating 8 m primary mirrors. Each will be derived from an 8.4 m blank. The most significant new requirement is for figuring the segments as off-axis segments of a large parent paraboloid. Fortunately, the stressed-lap method being used to make the on-axis 8.4 m mirrors at f/1.1 for the LBT is readily adapted for off-axis figuring. The segment and 1.2 m polishing tool will be driven with the same motions as for an axisymmetric piece, but the algorithm that controls the tool's shape as it moves will be modified to fit the off-axis figure. The existing tool can accommodate shape variations for a 20/20 segment, no larger than those for the 6.5 m mirrors for the MMT and Magellan telescopes already figured to the diffraction limit at f/1.25 (Martin et al. 1998, Martin et al. 2000). The greater asphericity of the 21 m f/0.7 parent is offset by its greater focal length.

Each segment will be supported from its back to a steel cell via a rigid hexapod (defining the six degrees of freedom) and flotation force actuators. The cells will be mounted to a steel structure with two primary beams on elevation C-rings, like the LBT mount. Displacements or relative motion of the off-axis segments caused by slow gravitational bending of the supporting structure with elevation will be corrected by adjustments to the hexapod arms. Appropriate mechanisms are already in use at the MMT and Magellan telescopes. To correct dynamic bending caused by wind gusts, the adaptive secondary mirror will be constructed with the same 7 segment geometry as the primary. Fast control of piston, tip and tilt that is possible at the secondary as well as higher order terms will then take care of any discontinuities at the primary petal boundaries.

3.2. Deformable Mirrors

The curved deformable mirrors used for the secondaries and clamshell conjugate mirrors will use the technology developed by Steward and Arcetri observatories for the MMT and LBT adaptive secondary mirrors (Wildi et al. 2001). The 64 cm convex hyperboloidal MMT secondary with 336 actuators is shown in Figure 5a. It was recently operated in the lab in closed loop about a Shack-Hartmann sensor, with simulated seeing, and recovered a stable corrected image shown in Figure 5b. Each 0.8 m segment of the 20/20 deformable secondaries will use a 2 mm thick glass facesheet with 672 voice-coil supports, conjugated to 30 cm spacing at the entrance pupil. The reference body underlying the 7 segments will be a single, rigid, scallop-edged piece of glass 2.3 m in diameter.

The curved deformable mirrors for the clamshell MCAO unit, 0.56 and 0.84 m diameter, conjugate to diameters of 28 m and 25 m at 12 and 6 km respectively. For correction at 0.5 m spacing at these layers, actuator spacings of 1 cm and 1.3 cm respectively will be required, with strokes of tens of microns to accommodate tilt and low order correction. The M4 mirrors will also be configured to allow piston motions of up to 1 mm. These are included to correct for tracking errors under conditions of gusting winds. Each mirror will provide $\frac{1}{2}$ the correction by moving by $\frac{1}{4}$ of the path error. A 1 mm path length error will require a 250 μm piston motion of each M4 mirror, and a corresponding refocus of 2 μm sagittal depth.
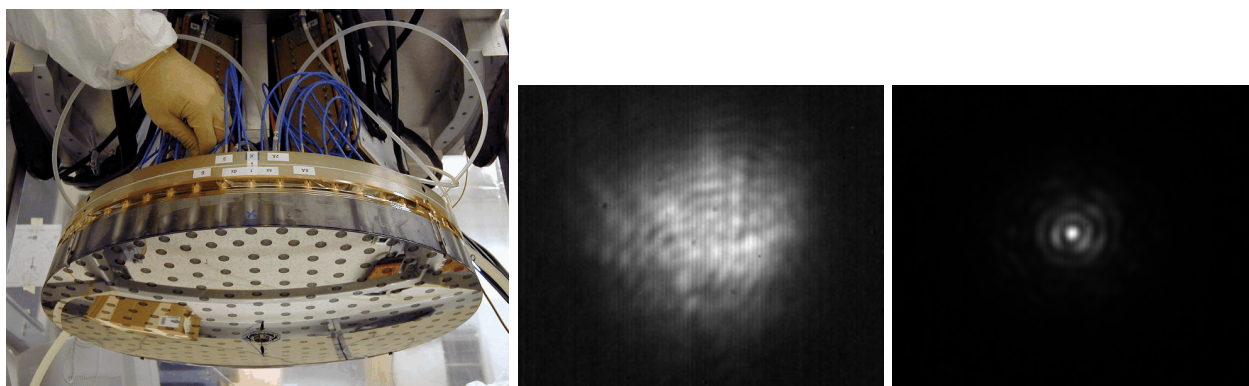

Figure 5. a) The MMT adaptive secondary mirror, prior to aluminization of the front surface, showing the 336 actuators. b) Images at 1.55 μm, with and without compensation, showing the first closed-loop result obtained in the lab. Dynamic phase aberration was introduced in the illuminating beam.

4. MCAO FOR 20/20; SIMULATIONS AND TEST AT THE 6.5 M MMT

MCAO is critical for the success of 20/20. To implement the tomographic wavefront sensing required to drive each telescope's three deformable mirrors, we plan to use five sodium laser guide stars. These will be launched from behind the secondary mirror, and pointed at the vertices of a regular pentagon on a radius of 1 arcminute.

In an MCAO system using lasers at only a single height, however, 3 NGS are required to avoid anisoplanatic effects associated with height uncertainty of quadratic wavefront errors (Brusa et al. 2000). Even for 20/20, with its large collecting area, it will not always be possible to identify 3 NGS in any chosen field. Five Rayleigh beacons will therefore be used to supplement the information from the higher-altitude sodium beacons. These will be launched and aimed in the same way as the sodium lasers. The use of lasers at two distinct heights will allow control of all three deformable mirrors without reference to more than a single natural guide star.

As a test of the geometry and the tomographic algorithm, we plan to build a scaled-down version of 20/20's MCAO system on the existing 6.5 m MMT. The 6.5 m primary is roughly one-third the diameter of 20/20's unit telescopes. The effect of sodium guide star lasers for 20/20 is therefore very well modeled by Rayleigh beacons placed at one-third the height of the sodium layer, or about 30 km. In both cases, rays from the five laser beacons will pass through the turbulence at the same angles on their way to the primary mirror, and the shear distances between beacon and star paths through a given layer of turbulence will thus be the same in both cases (Figure 6).
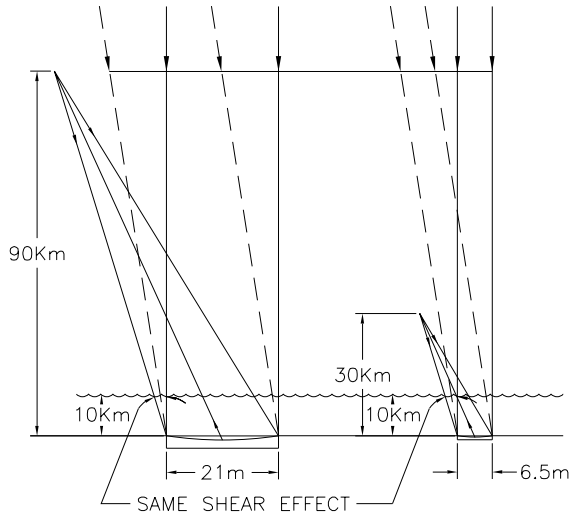
Because of the very small depth of focus of a 21 m aperture, even sodium beacons will not remain in focus as the light traverses the sodium layer. One is forced then to a pulsed beam format, and to avoid wasting most of the resonance photons through range gating, the pulses must be tracked dynamically in focus. The range of motion in the focal plane though is very small for sodium—no more than 0.2 mm in an f/1 beam. On the other hand, for Rayleigh beacons, there is enormous potential to increase the brightness of the beacon by collecting light over a wide range of height, which requires a refocuser with greater range of motion (Angel 2000, Angel & Lloyd-Hart 2000). We are already building such a device, which will be used with the Rayleigh beacons on the MMT (Lloyd-Hart et al. 2001).

Figure 6. Geometry of 20/20's LGS and the correspondence with the planned test at the 6.5m MMT.

Preliminary numerical simulations have been carried out of our planned MCAO scheme on both telescopes. The beacon geometries used in the models are summarized in the table below. Corrections were applied only at the first two mirrors, conjugated to 0 and 6 km. Future simulations will include all 3 DMs, and a number of different model atmospheres.

	MMT			20/20		
	Number	Field angle	Focus range	Number	Field angle	Focus range
Low-altitude LGS	5	1 arcmin	16—20 km	5	1 arcmin	20—30 km
High-altitude LGS	5	1 arcmin	20—30 km	5	1 arcmin	92—97 km

Wavefronts from each of the laser beacons were assumed to have been reconstructed from individual WFS measurements as vectors of Zernike polynomial amplitudes. Noise corresponding to WFS read noise and photon noise was added to each Zernike amplitude. A single vector containing all the individual wavefronts was then multiplied by the tomographic reconstructor matrix to obtain an estimate of the Zernike amplitudes required on each of the two DMs. The phase maps from each mirror were computed on a point-by-point basis along 49 different lines of sight from the optical axis out to a field angle of 1 arcminute. The corresponding atmospheric phase maps, representing the wavefront error that would be accumulated by starlight from these directions, were computed in these same directions. The difference between the atmospheric and DM phase maps was taken, and a Strehl ratio computed for each direction.
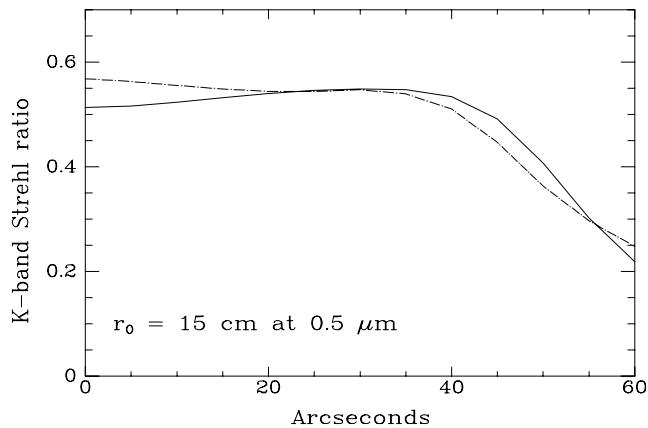

The tomographic reconstructor R was a maximum a posteriori probability estimator (Flicker et al. 2000), based on the assumed Kolmogorov statistics of the modeled atmosphere:

$$R = (G^T C_N^{-1} G + C_A^{-1})^{-1} G^T C_N^{-1} \quad (1)$$

where G is the interaction matrix relating Zernike modes applied to the DMs to the modal amplitudes measured by each of the beacons, and C_N and C_A are respectively the covariance matrices of the modal noise and amplitudes. In the case of the MMT, 100 modes per DM were corrected, while the 20/20 model corrected 1000 modes per DM. The 7-layer Cerro Pachon model atmosphere (Flicker et al. 2000) was used.

Figure 7. K-band Strehl ratio computed from numerical simulations of 2-DM MCAO at 20/20 (solid line) and the MMT (dashed line)

The results of the simulations are shown in Figure 7 in terms of Strehl ratio in the K band. We find we can recover a field 80 arcsec in diameter corrected to $> 50\%$ Strehl ratio. Almost full sky coverage is obtainable in this mode, and not only in the K band modeled here. In contrast to the single conjugate case, with MCAO the size of the corrected field remains approximately constant with wavelength. In the case of 20/20 then, we can expect full sky coverage even at the shortest corrected wavelengths.

5. ACKNOWLEDGMENTS

REFERENCES

Angel R., "Dynamic Refocus for Rayleigh Beacons," *Science with the LBT*, ed. T. Herbst, Sponsored by the Max-Planck Society and the LBT Beteiligungsgesellschaft, Proceedings of a Workshop held at Ringberg Castle, Bavaria, 21-25, July 2000.

Angel J. R. P., Hill J. M., Strittmatter P. A., Salinari P., and Weigelt G., "Interferometry with the Large Binocular Telescope," *Astronomical Interferometry*, ed. R. D. Reasenberg and J. B. Breckinridge, SPIE **3350**, 881, 1998.

Angel R. and Lloyd-Hart M., "Atmospheric tomography with Rayleigh laser beacons for correction of wide fields and 30 m class telescopes," *Adaptive Optics Systems and Technology*, ed. P. Wizinowich, SPIE **4007**, 270, 2000.

Bertero B. and Boccacci P., "Image restoration methods for the Large Binocular Telescope (LBT)," *Astron. Astrophys. Suppl.*, **147**, 323, 2000.

Brusa G., Riccardi A., Esposito S., Femenia B., and Carbillet M., "A study for a multi-conjugate AO system for 8 m class telescope," *Laser Weapons Technology*, ed. T Steiner, P Merritt, SPIE **4034**, 2000.

Correia S. and Richichi A., "Interferometric imaging tests for the Large Binocular Telescope," *Astron. Astrophys. Suppl.*, **141**, 301, 2000.

Del Vecchio C., Miglietta L., and Davison W., "The mechanical design of the Large Binocular Telescope," *Advanced Technology Optical Telescopes V*, SPIE, **2199**, 773, 1994.

Esposito S., Riccardi A., and Femenia B., "Differential piston angular anisoplanatism for astronomical optical interferometers," *Astron. and Astrophys.*, **353**, L29, 2000.

Flicker R., Rigaut F., and Ellerbroek B., "Comparison of multiconjugate adaptive optics configurations and control algorithms for the Gemini-south 8-m telescope," *Adaptive Optical Systems Technology*, SPIE, **4494**, 1032, 2000.

Hege E. K., Beckers J. M., Strittmatter P. A., and McCarthy D. W., "The Multiple Mirror Telescope as a phased array telescope," *Appl. Opt.*, **24**, 2565, 1985.

Hege E. K., Christou J. C., Jefferies S. M., and Cheselka M., "Technique for combining incoherent interferometric images," *J. Opt. Soc. Am A*, **16**, 1745, 1999.

Lloyd-Hart M., Georges J., Angel R., Brusa G., and Young P., "Dynamically refocused Rayleigh laser beacons for atmospheric tomography," *Adaptive Optics Systems and Technology II*, SPIE **4494**, 2001.

Martin H. M., Allen R. G., Angel J. R. P., Burge J. H., Davison W. B., DeRigne S. T., Dettmann L. R., Ketelsen D. A., Kittrell W. C., Miller S. M., Strittmatter P. A., West S. C., "Fabrication and measured quality of the MMT primary mirror," *Advanced Technology Optical/IR Telescopes VI*, ed. L. M. Stepp, SPIE **3352**, 194, 1998.

Martin H. M., Allen R. G., Cuerden B., DeRigne S. T., Dettmann L. R., Ketelsen D. A., Miller S. M., Parodi G., Warner S., "Primary mirror system for the first Magellan telescope," *Optical Design, Materials, Fabrication, and Maintenance*, ed. P. Dierickx, SPIE **4003**, 2, 2000.

Shao M. and Colavita M., "Potential of long baseline infrared interferometer narrow angle astronomy," *Astron. and Astrophys.*, **262**, 353, 1992.

Wildi F., Brusa G., Riccardi A., Allen R., Lloyd-Hart M., Miller D., Martin B., Biasi R., Gallieni D., "Progress of the MMT adaptive optics program," *Adaptive Optics Systems and Technology II*, SPIE **4494**, 2001.

Woolf N. and Ulich B. L., "Gone with the wind, or sailing and seeing with a giant telescope," in *Site Testing for Future Large Telescopes*, ed. A. Ardeberg and L. Woltjer, ESO, 163, 1984.